



## Synthesis and Characterization of ZnO Nanoparticles in Presence of Triethanolamine (TEA) as Surfactant *via* Sol-Gel

Maroof A. Hegazy,<sup>a</sup>, Hayat H. El-Agamy,<sup>b,\*</sup>



<sup>a</sup>Nano Technology Unit, Solar and Space Research Department, National Research Institute of Astronomy and Geophysics (Nano NRIAG), 11421 Helwan, Cairo, Egypt

<sup>b</sup>Nuclear Materials Authority (NAM), El Katameya, Cairo, Egypt

### Abstract

Zinc oxide (ZnO) nanoparticles have a great interest due to their important electrical and optical properties that have the potential to bring benefits to many areas of research and application. The present study is the preparation of zinc oxide nanoparticles using Sol-gel chemical method and the preparation using surfactant. The surfactant used was triethanolamine (TEA). Surfactant and unsurfactant ZnO nanoparticles were prepared to accomplish a comparative study. The properties of the prepared ZnO NPs have been characterized with the aid of many analytical techniques including Transmission electron microscopy (TEM), Fourier transform infrared spectroscopy (FT-IR), X-ray diffraction (XRD) and UV-Vis spectroscopy. The surfactant used was triethanolamine (TEA). The obtained ZnO NPs were spherical with average size of 79 nm without agglomeration. FTIR spectra showed the adsorption of TEA on the ZnO surface. The results of the UV-vis studies showed a decrease in band gap energy of 2.23eV as compared with the unsurfactant value of ZnO (3.28eV). Surfactant ZnO nanoparticles showed larger crystallite size and smaller bandgap in contrast to unsurfactant ZnO nanoparticles. TEA can use for prepare of nanomaterials with different properties for specific applications.

**Keywords:** Zinc oxide nanoparticle; Triethanolamine (TEA); Sol-gel; Surfactant; band gap.

### 1. Introduction

Metal oxides play a very significant role in many aspects of chemical, physical and material science [1-4]. In recent years, ZnO nanoparticle has found widespread interest due to its many exciting properties. For instance, it has a wide direct band gap (3.37 eV) and a large exciton binding energy of 60 meV at room temperature. Moreover, it has excellent chemical and thermal stability [5]. It is used in many applications such as solar cells, gas sensors [2-8], LEDs, piezoelectric devices, thin film transistors, laser and optoelectronic devices [9,10].

ZnO nanoparticle can be prepared by various methods such as hydrothermal, precipitation, spray pyrolysis, thermal decomposition and sol-gel method. The sol-gel method is more popular due to their advantages such as low temperature and process control. Moreover, this method shows good optical properties and simple, but this can be carried out only by good control of the size and shape of the particles [11].

Organic surfactants are used to acquire the desired size and morphology. In addition, organic surfactants prevent the agglomeration of particles and superior optical properties. Organic surfactant such as PVP [12], CTAB [13], thiophenol [14,15], TEA [16], starch [17], and glucose [18]. TEA is as surfactant which is both a tertiary amine and a triol with a lone pair of electrons on the nitrogen atom [19]. TEA is used in industrial milling to prevent agglomeration and in cosmetic and food products due to has good dissolution ability, low cost, and available. In this study we report the change in the properties of ZnO nanoparticles with adding of TEA synthesized by sol-gel method. The structural, morphological and optical properties were studied.

### 2. Experimental Details

#### 2.1. Reagent

Zinc sulphate heptahydrate (M=287.49g/mol), and KOH were obtained from Sigma-Aldrich. Triethanolamine used as a surfactant and ethanol used as solvent were purchased from Merck Chemical Reagent Company without further purification.

\*Corresponding author e-mail: [hayatrock97@hotmail.com](mailto:hayatrock97@hotmail.com); (Hayat H. El-Agamy).

Receive Date: 30 December 2020, Revise Date: 06 January 2021, Accept Date: 15 January 2021

DOI: 10.21608/EJCHEM.2021.55874.3189

©2021 National Information and Documentation Center (NIDOC)

## 2.2. Preparation of ZnO Nanoparticle by sol-gel

- (A) ZnO nanoparticles were synthesized by dissolving 0.2 M zinc sulphate heptahydrate in 100 ml ethanol by continuous stirring for half an hour until a clear solution is obtained then suitable amount of KOH solution was added to get pH 9 at a temperature of 60 °C for 2 hours. The colloidal precipitate obtained was cooled and washed with D.I water and ethanol several times, then dried at 70 °C for 2 hours. The dried gel form was calcined at 900°C for 2 hours by using a muffle furnace.
- (B) The latter steps were repeated using 5 ml of TEA (Triethylamine) as surfactant stabilizer.

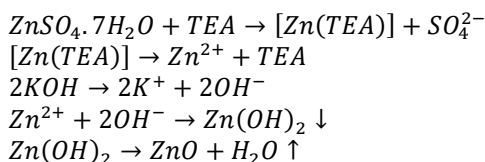
## 2.3. Characterization of ZnO powder

Morphological feature and particle size of the as-synthesized samples were examined by high resolution transmission electron microscope (HRTEM) (Philips (3M200)) and Particle size distribution of the zinc oxide particles was also measured by using a laser based particle size analyzer (Malvern-3000, Mastersizer, and Japan) and the average particle size was studied from the TEM images using software such as Image J and Origin.

The crystalline phases of the as-synthesized samples were identified by X-ray diffraction analyzer (Shimadzu XRD-6000, model D/Max-IIIB, the accuracy is 0.001o) using Cu K $\alpha$  radiation ( $k = 0.15418$  nm) and the composition of the synthesized ZnO nanoparticles were determined by using Fourier transform infrared (FTIR) spectroscopy was performed using Bruker (Vector 22) instruments. The ultraviolet–visible (UV–Vis) absorption spectra were recorded on a UV– Vis scanning spectrophotometer (Thermo Scientific, Japan).

## 3. Result and Discussion

TEA (N (CH<sub>2</sub>CH<sub>2</sub>OH) <sub>3</sub>) has a single lone pair of electrons on the nitrogen atom, due to which it generally acts as a weak base. The possible reactions for the precipitation of ZnO nanoparticles in the presence of TEA and KOH can be depicted as:



In the Sol-gel case, the amine group of TEA binds to surface ZnO atoms, while the OH groups provide hydrophilicity [20,21]. The TEA molecules passivate the surface and create a steric barrier between neighboring ZnO nanoparticles. A schematic representation of capped ZnO nanoparticles is shown in figure 1.

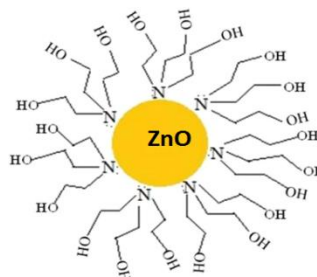


Fig. 1. A schematic representation of capped ZnO nanoparticles.

KOH is thought to be better than NaOH, because K<sup>+</sup> has a larger ion radius and so a lower chance of including into the ZnO lattice [22-23]. What's more, some say that K<sup>+</sup> is attracted by the OH<sup>-</sup> around the nanocrystal and forms a virtual capping layer, this way stopping the nanocrystal growth [24].

### 3.1. X-Ray Diffraction (XRD) studies

The crystallite size of the crystals was calculated using the broadening of the diffraction lines corresponding to the maximum peak intensity by the Scherrer formula (1).

$$D = 0.9\lambda / (\beta \cos \theta) \quad (1)$$

Where D is the diameter of the crystallites of the crystals,  $\lambda$  is the wavelength of CuK $\alpha$  line (0.15406 nm),  $\beta$  is full width at half maximum (FWHM) in radian and  $\theta$  is Bragg angle.

The XRD patterns for both powders in figure 2 (A, B) showed that the ZnO nanoparticles for both powders are crystalline in nature [25].

The peaks of the XRD patterns for both synthesized zinc oxide powders corresponded to the (100), (002), (101), (102), and (110) planes. All the XRD results approved that the synthesized powders in this study consisted of single-phase hexagonal wurtzite ZnO. Although both powders showed XRD patterns that indicated that they include ZnO, the peak intensities for both powders were different. The peak intensity for ZnO powder without TEA was higher than that of the ZnO powder with TEA.

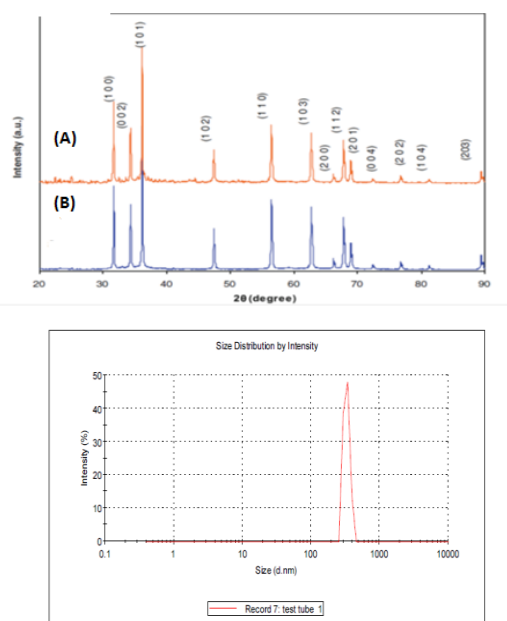


Fig. 2. (A, B). XRD pattern of the ZnO powders synthesized without using TEA (A) and using TEA (B).

Based on the Scherrer formula, the average diameters of the ZnO crystallites for the ZnO (A) and ZnO (B) powders were calculated to be 11 and 58 nm, respectively.

### 3.2. FTIR absorption studies

FTIR spectra figure 3 (A, B) investigated the formation of ZnO nanoparticles and the presence of several chemical functional groups.

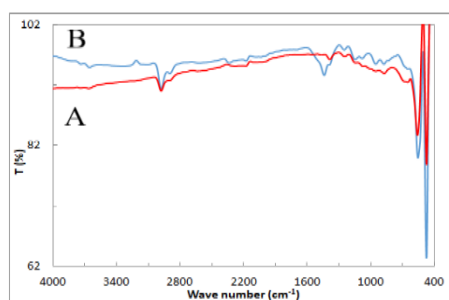


Fig. 3. (A, B) FTIR spectrum of ZnO nanoparticles (A) prepared without using TEA and (B) ZnO prepared with using Triethanolamine.

The peak at 1,350  $\text{cm}^{-1}$  in the case of capped ZnO may be from C–H<sub>2</sub> in TEA [26]. The peaks at 450 and 530  $\text{cm}^{-1}$  was observed for each ZnO nanoparticles are

investigated stretching vibration of Zn–O bond. As can be seen ZnO nanoparticles extracted from suspensions with TEA have two other peaks around 2850 and 2950  $\text{cm}^{-1}$  attributed to CH bond of TEA or H+TEA ions [27].

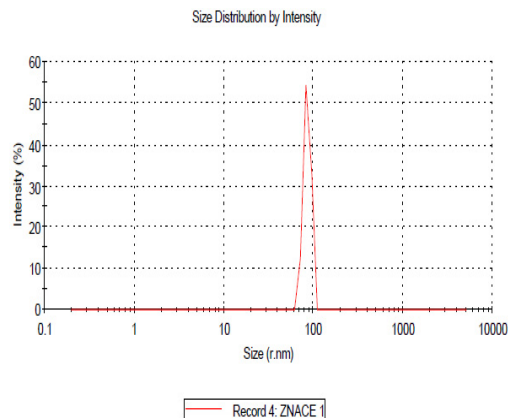
### 3.3. Dynamic light scattering analysis

Dynamic light scattering was utilized for detection the average hydrodynamic size of the synthesized ZnO nanoparticles. The size determined by DLS was detected to be much larger than the size determined by XRD and TEM. DLS detected the hydrodynamic radius of the particle whereas by TEM we obtained an estimation of the projected area diameter.

Fig. 4. Size distribution by intensity of ZnO nanoparticles prepared via sol-gel with Triethanolamine.

Fig. 5. Size distribution by intensity of ZnO nanoparticles prepared via sol-gel without Triethanolamine.

The Malvern Zetasizer is used to measure the particle size in the colloidal solution of ZnO NPs dispersed in water. The size distribution remains in



narrow range as shown in figure 4, 5. The particle size of synthesized ZnO powder is about 84.98 nm in with TEA figure (4) While with average size ranging from 250 to 500 nm were observed for without TEA figure (5).

When a dispersed particle moves through a liquid medium, a thin layer of the solvent adheres to its surface. This layer affects the movement of the particle in the medium, thus the hydrodynamic diameter confers us information of the inorganic core along with any coating material and the solvent layer linked to the particle as it moves under the effect of Brownian motion. While concluding size by TEM, this hydration layer is not present hence, information is obtained only about the inorganic core.

### 3.4. TEM morphology of the nanoparticles

The surface morphologies and particle diameters of ZnO synthesized by sol-gel with and without TEA were investigated using TEM.

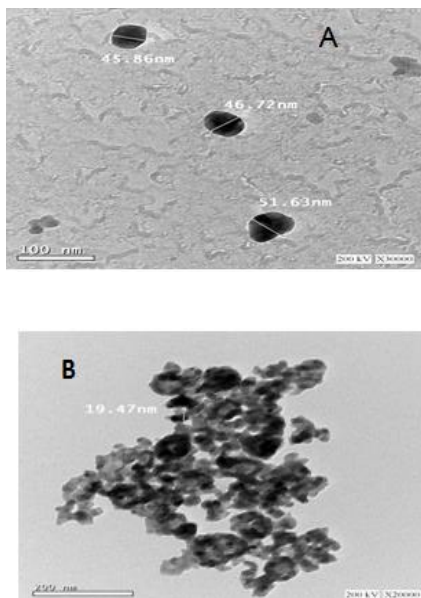


Fig. 6. (A, B) TEM images of ZnO powders synthesized (a) with using TEA and (b) without using TEA.

The TEM images of ZnO powders synthesized by Sol-gel and precipitation are showed in figure 6 (A, B). Sol-gel method using TEA favored the formation of uniform spherical-shaped nanoparticles of size 45-50 nm is a single-phase nanoparticle (not agglomerate) (Figure 6 A), while without using TEA led to the formation of agglomerate with spherical-shaped which morphology had length up to 200 nm (Figure 6 B).

The surfactant played a significant role in the growth mechanism of ZnO nanoparticles. The surfactant on the surface of ZnO plays two roles: firstly, it helps reduce the defects in nanocrystals during nucleation and secondly, it attaches to the surface of nanoparticles so as to effect on the size of the particles. Results from the TEM analysis indicate that the particle sizes in both Powders were larger than the crystallite sizes determined from the XRD patterns. The observed particles consisted of single primary nanocrystallites and secondary ZnO particles formed by the fusion of several primary crystallites. Thus, ZnO primary crystallite aggregation constructed the larger polycrystalline particles observed in TEM [28,29]. Furthermore, it can be seen that without and

with using TEA to histograms the average diameter of ZnO nanoparticles are 20 and 40 nm, respectively.

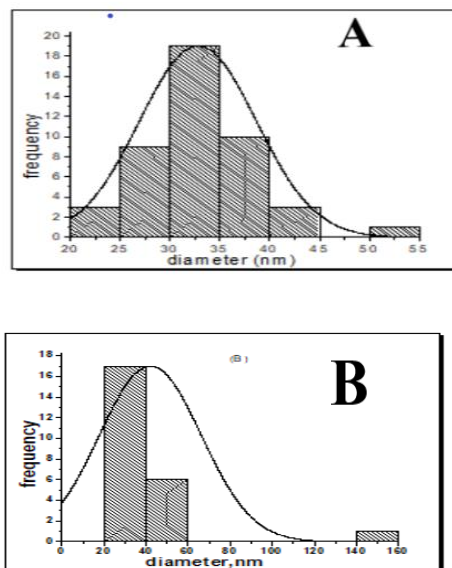
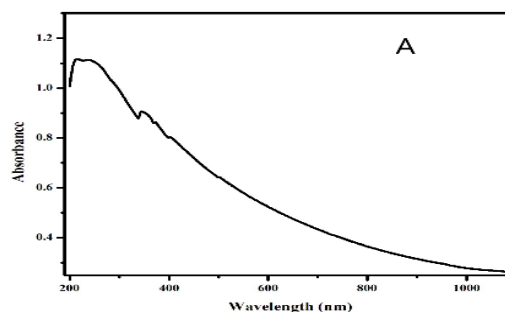


Fig. 7. (A, B) Size distribution histograms of ZnO nanoparticles without and with TEA

### 3.5. UV-Visible Spectrophotometer

The effect of the preparation method on the photo-optical of the zinc oxide nanoparticles were studied through their capability of absorbing the UV radiation. The spectra of the UV-Visible absorption by the Zinc oxide nanoparticles; both ZnO NPS A (without Triethanol amine) and ZnO NPs B (with Triethanol amine), are shown in Figure 8. Both A and B have shown an absorption band at blue shift area (less than 400nm). About the absorption spectra, the effective wavelengths of ZnO nanoparticles A (without Triethanol amine) and B (with Triethanol amine) are 265 and 380 nm, respectively.



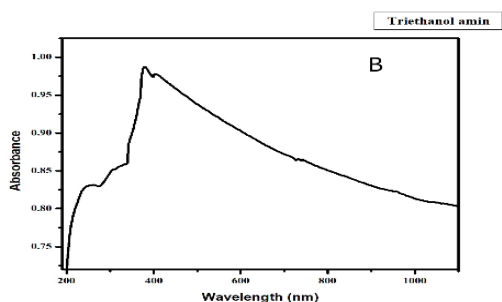


Fig. 8. Electronic absorption of UV-VIS spectra for ZnO nanoparticles A and B.

In line with, respective energy band gaps of 3.28 and 2.23 eV for sample A and B were detected in Figure 9. The direct band gap of ZnO is estimated from the plot of  $(\alpha h\nu)^2$  versus  $h\nu$ , where  $h\nu$  is the photon energy and  $\alpha$  is the ratio of the absorption coefficient to the scattering coefficient. These band gaps can explicitly ensure the blue shift which had occurred for the prepared ZnO owing to the inverse proportion of energy gap and wavelength.

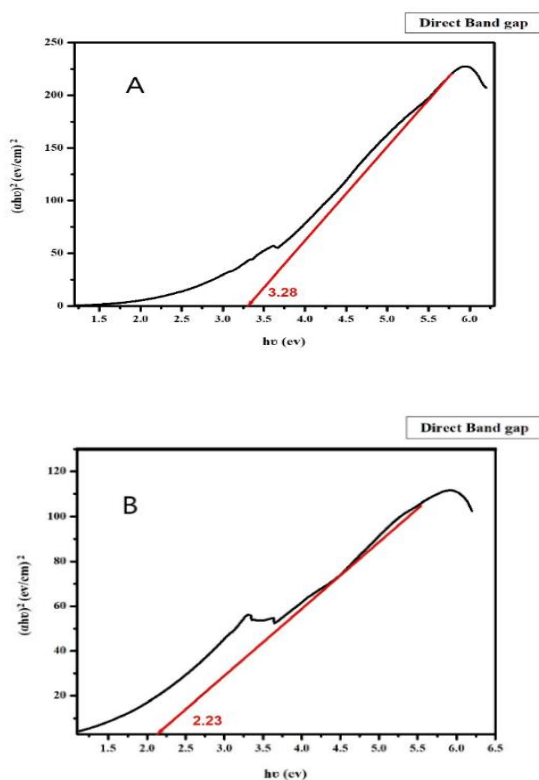


Fig. 9. The band gap for ZnO nanoparticles A and B.

From other studies was found that the band gap of pure ZnO is  $\sim 3.3$  eV which is good agreement with ZnO nanoparticles A, but the optical band gap of ZnO nanoparticles B decreases with increasing crystallite

size and vice versa [30-32]. This surface plasmon resonance band undergoes a red- or blueshift, depend on the quantum size effects. The absorbance of ZnO NPs depends on the influence of various factors such as physical parameters (size and pH), carrier concentrations, the presence of oxygen vacancies and shape. Large band gap energy and highly blue shifted absorption edge confirm that the prepared ZnO nanoparticle show strong quantum confinement effect.

#### 4. Conclusions

In this work ZnO nanoparticles were synthesized by sol-gel method without and with using surfactant lead to change in the particle size and shape of nanoparticles. According to the characterization results it is clear that by with using a surfactant (TEM) the particle agglomeration is very less and also the particle separation is good. Morphological investigations confirmed the formation of various nanostructures with variation in shape, size and aspect ratios, crystallinity, and lattice arrangements. The synthesized ZnO average particle size is calculated as 30 nm by using Scherrer's formula. The TEM image showed spherical shape nanoparticle formed with diameter range 50 nm. Whereas, without using a surfactant particle size is diameter range 200 nm. FTIR studies showed the adsorption of TEA on the surface of ZnO nanoparticles. Overall decreasing nature of optical band gap (from 3.28 eV to 2.22 eV) has been showed in ZnO with using triethanolamine. (Upon using TEA, decrease in the optical band gap from (3.28 eV to 2.22 eV) was shown in ZnONPs.

#### 5. References:

- [1] Ezzat H. A., Gomaa I., Gawad A. A., Osman O., Mahmoud A. A., Sleim M., Elhaes H., Ibrahim M. A., Semiempirical Molecular Modeling Analyses for Graphene/Nickel Oxide Nanocomposite, Letters in applied NanoBioScience, 9, 1459 – 1466, (2020).
- [2] Badry R., Ibrahim A., Gamal F., Shehata D., Ezzat H., Elhaes H., Ibrahim M., Electronic Properties of Polyvinyl alcohol/ TiO<sub>2</sub>/SiO<sub>2</sub> Nanocomposites, Biointerface Research of Applied Chemistry, 10, 6427-6435, (2020).
- [3] Ezzat H. A., Hegazy M. A., Nada N. A., Ibrahim M. A., Effect of Nano Metal Oxides on the Electronic Properties of Cellulose, Chitosan and Sodium Alginate, Biointerface Research in Applied Chemistry, 9, 4143-4149 (2019).
- [4] Ezzat H. A., Hegazy M. A., Nada N. A., Ibrahim M. A., Application of Natural Polymers Enhanced with ZnO and CuO as Humidity Sensor, NRIAG Journal of Astronomy and Geophysics, 9, 586-597(2020).

- [5] Lou X., The Development of ZnO series ceramic semiconductor gas sensors, *Journal of Transducer Technology*, 3, 1-5, (1991).
- [6] Wang Z. L., Ten years' venturing in ZnO nanostructures: from discovery to scientific understanding and to technology applications, *Chinese Science Bulletin*, 54, 4021 (2009).
- [7] Elhaes H., Ezzat H., Badry R., Yahia I.S., Zahran H.Y., Ibrahim M.A., The Interaction Between Carbon Nanotube Decorated with CuO and ZnO and Hydrogen, *Sensor Letter*, 16, 445 – 453 (2018).
- [8] Elhaes H., Ezzat H., Morsy M., El-Khodary S.A., Yahia I.S., Zahran H.Y., Ibrahim M.A., PVC/ZnO nanocomposite as gas sensor for natural gas, *Sensor Letter*, 16, 513-516 (2018).
- [9] Huang M. H., Mao S., Feick H., Yan H. Q., Wu Y. Y., Kind H., Weber E., Russo R., Yang P. D., Room-Temperature Ultraviolet Nanowire Nanolasers, *Science*. 292, 1897-1899 (2001).
- [10] Govender K., Boyle D. S., O'Brien P., Binks D., West D., Coleman D., Room-Temperature Lasing Observed from ZnO Nanocolumns Grown by Aqueous Solution Deposition, *Advanced Materials*, 14, 1221-1224 (2002).
- [11] Kim Y.S., Tai W.P., Shu S.J., Effect of preheating temperature on structural and optical properties of ZnO thin films by sol-gel process, *Thin Solid Films*. 491, 153-160 (2005).
- [12] Park W. I., Yi G. C., Electroluminescence in n- ZnO Nanorod Arrays Vertically Grown on p- GaN, *Advanced Materials*, 16, 87-90 (2004).
- [13] Mao D. S., Wang X., Li W., Liu X. H., Li Q., Xu J. F., Electron field emission from hydrogen-free amorphous carbon-coated ZnO tip array, *Journal of Vacuum Science and Technology B*, 20, 278 (2002).
- [14] Zhu Y. W., Zhang H. Z., Sun X. C., Feng S. Q., Xu J., Zhao Q., Xiang B., Wang R. M., Yu D. P., Efficient field emission from ZnO nanoneedle arrays, *Applied Physics Letters*, 83, 144 (2003).
- [15] Liu L., Zhang Y., Li C., Cao J., He Er, Wu X., Wang F., Wang L., Facile preparation PCL/ modified nano ZnO organic-inorganic composite and its application in antibacterial materials, *Journal of Polymer Research*, 27, 78 (2020).
- [16] Wang W. Z., Zeng B. Q., Yang J., Poudel B., Huang J.Y., Naughton M. J., Ren Z. F., Aligned Ultralong ZnO Nanobelts and Their Enhanced Field Emission, *Advanced Materials*, 18, 3275-3278 (2006).
- [17] Wang Z.L., Splendid One-Dimensional Nanostructures of Zinc Oxide: A New Nanomaterial Family for Nanotechnology, *ACS Nano*, 2, 1987-1992 (2008).
- [18] Chaari M., Matoussi A., Electrical conduction and dielectric studies of ZnO pellets, *Physica B: Condensed Matter*, 407, 3441-3447 (2012).
- [19] Sun C., Xue D., Tailoring Anisotropic Morphology at the Nanoregime: Surface Bonding Motif Determines the Morphology Transformation of ZnO Nanostructures, *The Journal of Physical Chemistry C*, 117, 5505-5511 (2013).
- [20] Lashkari M., Ghashang M., Preparation of thiazolidin-4-one derivatives using ZnO-NiO-NiFe<sub>2</sub>O<sub>4</sub> nanocomposite system, *Research on Chemical Intermediates*, 24, 1-9 (2020).
- [21] Demianets L. N., Kostomarov D. V., Kuz'mina I. P., UPushko S. V., Mechanism of growth of ZnO single crystals from hydrothermal alkali solutions, *Crystallography Reports*, 47, S86 (2002).
- [22] Yamabi S., Imai H., Growth conditions for wurtzite zinc oxide films in aqueous solutions, *Journal of materials chemistry*, 12, 3773-3778 (2002).
- [23] Liu B., Zeng H. C., Room Temperature Solution Synthesis of Monodispersed Single-Crystalline ZnO Nanorods and Derived Hierarchical Nanostructures, *Langmuir*, 20, 41964204 (2004).
- [24] Mohammed H. I., Giddings D., Walker G. S., Thermophysical properties of the nano-binary fluid (acetone-zinc bromide-ZnO) as a low temperature operating fluid for use in an absorption refrigeration machine, *Heat and Mass Transfer*, 56, 1037-1044 (2020).
- [25] Md A. H., Mahalakshmi S., Effect of Triethanolamine on Zinc Oxide Nanoparticles, *Materials Focus*, 2, 469-474 (2013).
- [26] Viswanatha R., Amenitsch H., Sarma D., Growth Kinetics of ZnO Nanocrystals: A Few Surprises, *Journal of the American Chemical Society*, 129, 4470-4475 (2007).
- [27] Kashyout A.B., Soliman H. M. A., Hassan H. S., Abousehly A. M., Fabrication of ZnO and ZnO: Sb nanoparticles for gas sensor applications, *Journal of Nanomaterials*, 2010, 341841 (2010).
- [28] Farrokhi-Rad M., Khanmohammadi Sh., Electrophoretic Deposition of Hydroxyapatite Nanoparticles from Different Alcoholic Suspensions: Effect of Triethanolamine, *ECS Transactions*, 82, 1 (2018).
- [29] Rani S., Suri P., Shishodia P.K., Mehra R. M., Synthesis of nanocrystalline ZnO powder via sol-gel route for dye-sensitized solar cells, *Solar Energy Materials and Solar Cells*, 92, 1639-1645 (2008).
- [30] Xu R., Zeng H. C., Self-generation of tiered surfactant superstructures for one-pot synthesis of Co<sub>3</sub>O<sub>4</sub> nanocubes and their close-and non-close-packed organizations, *Langmuir*. 20, 9780-9790 (2004).
- [31] Doris S., Johannes G., Robin K. T., Vassil V., Wolfgang P., Analysis of optical absorbance spectra for the determination of ZnO nanoparticle size distribution, solubility, and surface energy, *ACS NANO*, 3, 1703-1710 (2009).
- [32] Bharat T. C., Shubhama, Mondala S., Gupta H. S., Singh P. K., Dasa A. K., Synthesis of doped zinc oxide nanoparticles: a review, *Materials Today: Proceedings* 11, 767-775 (2019).